Mater. Res. Soc. Symp. Proc. Vol. 849 © 2005 Materials Research Society KK8.6

Large Scale Engineered Nanostructured Surfaces by Reactive Ion Etching with Kinetically Self-Assembled Non-continuous Metal Film as Etching Mask

Wei Wei[1,3], Mark Bachman[2,3], and Guann-Pyng Li[1,2,3]
[1.]Department of Chemical Engineering and Materials Science
[2.]Department of Electrical Engineering and Computer Science
[3.]Integrated Nanosystems Research Facilities, Henry Samueli School of Engineering
University of California, Irvine
Irvine, California 92697

ABSTRACT

In this study, we explored the possibility of using annealed non-continuous metal film enabled etching technique to produce large nano-structured surfaces. Non-continuous Ag film is deposited on silicon wafer with a thin layer of silicon dioxide using E-beam deposition, and then vacuum thermal annealing was applied on the deposited films, causing nano-scaled Ag particles to migrate and agglomerate into self-assembled islands of larger nanometer dimensions. We controlled the density and average size of the metal islands through thickness of the initial film and subsequent annealing rates. Reactive ion etching through the metal islands mask into the underneath silicon dioxide layer was performed following the annealing process. Preliminary hydrophobicity experiments were carried out using the engineered nano-structured surfaces.

INTRODUCTION

The fabrication of nano-structured surfaces of different materials is of broad interest in recent years not only because of its fundamental aspects but also because of a variety of potential applications that may be enabled. In microfuidic systems, surface properties strongly affect flow resistance since the surface-to-volume ratio is huge under this scenario. Nanostructured surfaces with certain degree of roughness were found to be surprisingly effective in reducing the surface friction and leading to a "water repellent" surface [1,2]. Nanopatterned surfaces also found innovative applications in recording cellular activities [3], protein recognition [4], which are the fundamental aspects for the future disease diagnosing and biological sensing. Another area that nanopatterned structures are finding increasingly important applications is the semiconductor quantum devices fabrication. Ordered arrays of silicon nanopillars and nanopoles [5-7] structures as field emission centers are explored since the discovery of strong visible photoluminescence from porous silicon by Canham [8]. Different techniques have been developed to obtain nanostructured surfaces in the last few years [9-13], such as swift heavy ion (SHI) irradiation [9] and spray deposition of nanoscale metal particles [10], anodization of aluminum thin film [11], polystyrene as metal deposition mask [7] and low power plasma with the presence of aluminum leads to the formation of AlF_3 as natural mask [5]. Nano-structured surfaces from size-selected clusters [12, 1], and e-beam lithography [13]. However, how to generate a large area of nanostructured surface for practical applications in a cost-effective manner is still a challenging issue.

It is well understood that thin layer metal films prepared by conventional deposition techniques, such as electron gun deposition, are always polycrystalline and non-continuous because of the crystal structure mismatch and wetting properties between the deposited materials and the substrate [14-20]. In the present study we explored the

possibilities of using non-continuous metal films as RIE etching mask to achieve large areas of different nanostructured surfaces in one single step. Vacuum thermal annealing technique was applied to the deposited metal films to adjust the film density and metal island size. As a result, the dimension of the etched nanostructures underneath and the interstitial size can be controlled accordingly. The ultimate goal of this work is to use this technique to prepare nanostructured surfaces for tuning surface properties between hydrophilic to hydrophobic for fluidic applications.

EXPERIMENTAL DETAILS

Silicon wafer with a thin layer of silicon oxide was used as substrate material. Before deposit metal film, the wafers were strictly cleaned using oxygen plasma, then rinsed with DI water, and finally blow-dried with N_2 gas. Silver was selected as the etching mask material since Ag is known to grow on this substrate via the formation of three-dimensional islands rather than in a layer-by-layer mode. Airco/Temescal CV-8 Electron-Beam Evaporator with deposition monitor IC6000 is introduced to deposit Ag film. The voltage applied to generate electron beam is 7.5 KV. The deposited film thickness is precisely controlled by controlling the deposition current less than 0.02 A. After materials deposition, the films were annealed in vacuum oven at 140 °C. Ag film morphology, island density, and the etched nano-structured surfaces were characterized using Scanning Electron Microscope (Hitachi 4700 Field Emission SEM with EDX, Hitachi, Japan) and Atomic Force Microscope (Multimode Scanning Probe Microscope, Veeco, USA). Reactive Ion Etching (Plasma-Therm Model 790, Plasma-Therm, USA) was implemented for the following etching process with CF_4+O_2 as etching gases. The isotropic/anisotropic etching properties can be adjusted by changing the gas ratio, chamber pressure and the RF power. The entire fabrication process is illustrated in Figure 1.

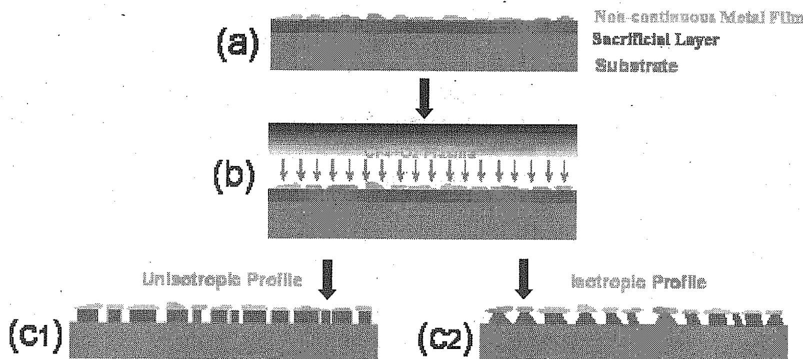

Fig 1. Process flow of nanopatterned surfaces. (a) A non-continuous metal deposited on silicon oxide wafer, (b) RIE etching through the metal film mask, (c) Two different etching profiles by varying process parameters, isotropic and unisotropic.

After etching, Ag film was removed using wet chemical etching process. Preliminary hydrophobicity experiments were carried out using the engineered nanostructured

surfaces we present here. A silicon dioxide wafer with flat surface was tested as a reference. Contact angles were measured with different surface conditions.

RESULTS AND DISCUSSION

Figure 2 shows SEM image of E-beam deposited Ag film. Individual Ag island in nanometer scale can be easily identified from the image. A major reason is accounted for the non-continuity or nonuniformity of metal films deposited through evaporation or sublimation mechanism [16, 18-20]: ion effect. Schuermeyer etc. [19, 20] experimentally observed that scattered electrons charge the floating substrate to a potential of many kilovolts in the E-Beam deposition process. This voltage accelerates positive metal ions toward the substrate and cause sputtering. Since the nonuniform nature of the electrical field generated between positive ions and floating substrate, deposited metal films are accordingly nonuniform.

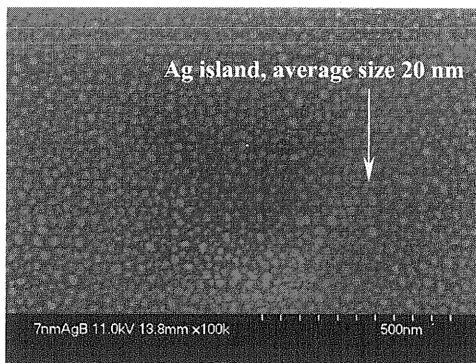

Fig. 2. SEM image of E-beam deposited 70 Å thick Ag film with average island size 20 nm and interstitial 25 nm.

Film thickness was measured at the film and substrate boundary using AFM as shown in Figure 3 (a). The thickness of the deposited film can be predicted theoretically from thermodynamic and kinetic theories, since the number of molecules leaving a unit area per second is given by [14]

$$N = N_0 \cdot \exp\left[-\left(\frac{\varphi_e}{kT}\right)\right] \qquad (1)$$

Where N_0 is a constant and function of T and φ_e, φ_e is the activation energy for evaporation, k is Boltzmann's constant, and T is temperature. From Figure 3 (b) it is easy to identify that relatively rough Ag film locates on the left hand side and smooth substrate on the right. Film under vacuum annealing at 140 °C for 1 hour was done and the SEM image of this film was given in Figure 4. Compared with Figure 2, the evidence of Ag islands growth can be identified. A preliminary estimation on the average Ag island size and interstitial size was carried out based on image processing technique. The average island size and interstitial size in Figure 2 was 20nm and 22nm respectively. For the same

film after 1 hour annealing as shown in Figure 4, the sizes are 25nm and 40nm respectively. A detail study on how the annealing process will affect Ag islands growth and agglomerate and quantitative evaluation will be carried out and not yet covered in this paper.

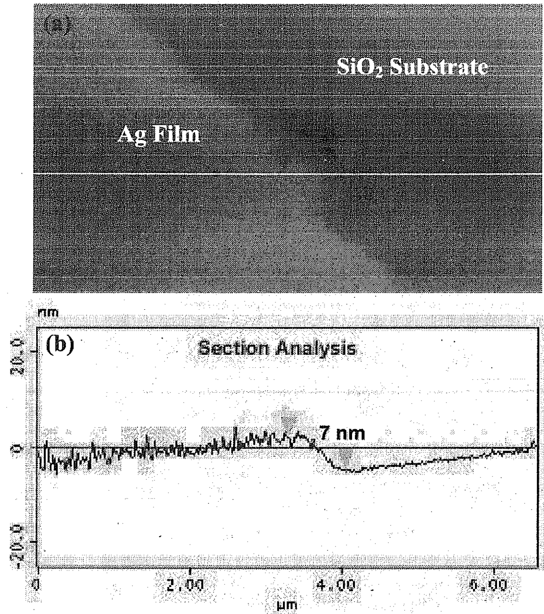

Fig. 3. (a) AFM image of Ag film and substratre boundary, film thickness was measured between the two marks on the image; (b) film thickness profile measurement.

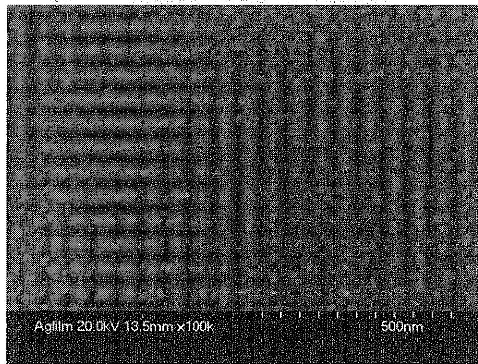

Fig. 4. SEM image of 70 Å Ag film after 1-hour annealing with average island size 25 nm and interstitial size 40 nm.

Reactive Ion Etching (RIE) is a powerful tool in micro-fabrication to achieve functional microstructures and devices. However, using RIE to achieve structures in nano-domain with new functionalities is not fully explored. Selective etching is one of the most important features that can be realized by RIE. The gases we use here to etch silicon oxide underneath the Ag islands are carbon CF_4 plus O_2 without attacking the Ag islands. As illustrated in Figure 1, the etching process is straightforward. However, in order to achieve different nanostructures underneath the Ag islands, such as nanopoles, nanocones, and nanopillars, the etching process need to be finely tuned. Etching time also need to be controlled in order to avoid over etch. Table 1 shows the experimental conditions and etching rate.

Table 1. RIE etching parameters and rate

CF4 flow (sccm)	O2 flow (sccm)	Chamber pressure (mTorr)	Power (W)	Etching rate (Å /Sec)
24	3	90	150	15

After RIE etching, Ag film was removed from the substrate using wet chemical etching. The obtained nanostructured surfaces were examined and characterized under SEM and AFM. Figure 5 shows SEM morphology of the etched surface with several Ag particles remain on the surface. Figure 6 is AFM image with section analysis of the etched surface. Pillar structures can be identified form the AFM image. A statistical evaluation was applied to analysis the average height of pillar structure, which is in the order of 25nm. The lateral dimension and average pillar-to-pillar distance were also determined as in the order of 22 nm and 45nm respectively. With respect to the effect of RIE undercut, the pillar-to-pillar distance is in good agreement with the interstitial size of the Ag islands mask.

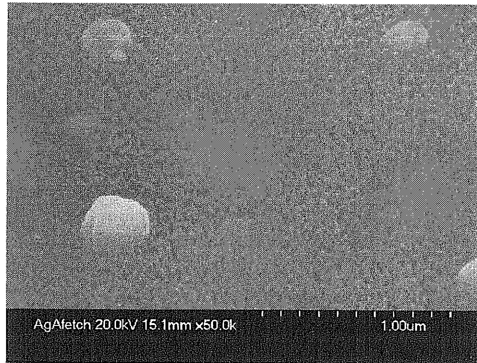

Fig. 5. SEM image of nanostructured surface after etching using non-continuous Ag film as etching mask

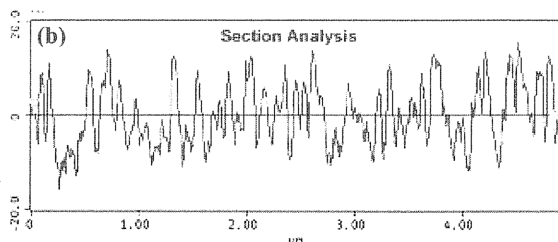

Fig. 6. AFM section analysis of etched surface with (a) 3D view and (b) surface height profile

Preliminary hydrophobicity experiments were carried out using the engineered nano-structured surfaces we present here. Flat silicon oxide surface was used as reference. Before contact angle measurement, both samples were surface treated using silane. Table 2 shows the measurement results. Obvious hydrophobicity enhancement can be achieved by using the nano-structured surface. Increased surface roughness is one of the major arguments that contribute to the enhanced surface hydrophobicity [21~23]. Future work will be directed in achieving surface hydrophobicity continuous adjustment by using the nano-structured roughened surface combined with different silane treatment.

Table 2. Surface contact angle measurement

Sample	Contact angle (deg)
#1 flat SiO_2	97
#2 Rough ENS*	126

* ENS stands for Engineered Nano-structured Surface.

CONCLUSIONS

In this study, we explored to use non-continuous metal islands as etching mask to generate nano-structured surface. Metal island sizes and interstitial size adjustment using vacuum annealing technique was demonstrated. Enhanced surface hydrophobicity was achieved using the engineered nano-structured surface.

REFERENCES

1. C. Cottin-Bizonne, J. L. Barrat, L. Bocquet, and E. Charlaix, Nat. Mater. **2**, 237 (2003).
2. J. Kim and C. J. Kim, Proc. IEEE Conf. MEMS, 2002, Las Vegas, Nevada, pp. 479-482.
3. O. D. Velev and E. W. Kaler, Langmuir. **15**, 3693 (1999).
4. H. Shi, W. B. Tsai, M. D. Garrison, S. Ferrari, and B. D. Ratner, Nature. **398**, 593 (1999).
5. M. Gotza, M. Dutoit, and M. Iiegemes, J. Vac. Sci. Technol. B. **16**, 582 (1998).
6. S. E. Huq, G. H. Grayer, S. W. Moon, and P. D. Prewett, Mater. Sci. Eng. B. **51**, 150 (1998).
7. A. Wellner, P. R. Preece, J. C. Fowler, and R. E. Palmer, Microelectron. Eng. **57**, 919 (2001).
8. L. T. Canham, Appl. Phys. Lett. **57**, 1046 (1990).
9. S. M. M. Ramos and E. Charlaix, Phys. Rev. E. **67**, 031604 (2003).
10. F. Schülz, S. Franzka, and G. Schmid, Adv. Funct. Mater. **12**, 532 (2002).
11. H. Masuda, and K. Fukuda, Science. **268**, 1466 (1995).
12. R. E. Palmer, S. Pratontep, and H. G. Boyen, Nat. Mater. **2**, 443 (2003).
13. S. Han, S. A. Yang, T. Hwang, J. Lee, J. D. Lee, and H. Shin, J. J. Appl. Phys. **39**, 2556, (2000).
14. I. Brodie, and J. J. Muray, *The Physics of Micro/Nano-Fabrication*, Plenum Press, New York (1992).
15. S. Kundu, S. Hazra, S. Banerjee, M. K. Sanyal, S. K. Mandal, S. Chaudhuri, and A. K. Pal, J. Phys. D: Appl. Phys. **31**, L73 (1998).
16. A. Zur, and T. C. McGill, J. Appl. Phys. **55**, 378 (1984).
17. N. Doraiswamy, G. Jayaram, and L. D. Marks, Phys. Rev. B. **51**, 10167 (1995).
18. W. Knauer, J. Appl. Phys. **62**, 841 (1987).
19. F. L. Schuermeyer, W. R. Chase, and E. L. King, J. Vac. Sci. Tehnol. **9**, 330 (1971).
20. F. L. Schuermeyer, W. R. Chase, and E. L. King, J. Appl. Phys. **42**, 5856 (1971).
21. R. N. Wenzel, Ind. Eng. Chem. **28**, 988 (1936).
22. A. B. D. Cassie, S. Baxter, Trans. Faraday Soc. **40**, 546 (1944).
23. R. H. Dettre, R.E. Johnson. Adv. Chem. Ser. **43**,136 (1963).